Supporting Information

Bartesaghi et al. 10.1073/pnas.1413165112

SI Experimental Procedures

XF24 Oxygen Consumption and Extracellular Acidification Rate Analysis. OCR and ECAR measurements were made using the XF24 Analyzer (Seahorse Bioscience) following the manufacturer's instructions. Briefly, when chemicals were used during the measurements, they were preloaded in the drug delivery system, and after measuring basal OCR and ECAR, compounds are added sequentially into the wells during the assay. The effect on OCR was measured after each compound addition. XF assay medium was low-buffered bicarbonate-free DMEM, pH 7.4 (Sigma; 5030). Chemicals used in this study were as follows: rotenone (Sigma; 8875), antimycin A (Sigma; 8674), oligomycin (Sigma; O4876), FCCP (Sigma; C2920), TMPD (Sigma; T3134), and ascorbate (Sigma; A4034).

Isolation of Mitochondria and Nuclear DNA. Dry pellets of 1×10^6 cells were resuspended in 200 μL of PBS and processed using a QIAamp DNA Mini Kit (Qiagen) according to the manufacturer's protocol. DNA was eluted in distilled water, keeping the final concentration in the range of 50–200 ng/μL. Relative quantification of mitochondrial DNA (mtDNA) content has been performed using quantitative RT-PCR (QPCR) amplification with specific primers and TaqMan MGB probes for mouse *ND1* (NADH dehydrogenase subunit I; mtDNA) and 18S rRNA (nuclear DNA) [TaqMan Assays; Applied Biosystems (AB)]. Thermal cycling was performed using the ABI PRISM 7300 Sequence Detector System (AB). Threshold cycle number (Ct) was calculated with the ABI PRISM 7300 Sequence Detector Software (Applied Biosystems). The threshold was set ordinarily at 10 times the SD above the mean baseline emission value for the first 12 cycles.

Immunoblotting. Whole-cell lysates were prepared by lysing cells in Laemmli buffer (1×) or modified RIPA buffer [20 mM Hepes, pH 7.9, 5 mM $MgCl_2$, 25% (vol/vol) glycerol, 1% Nonidet P-40, 150 mM NaCl, 1× PhosphoSTOP, and 1× Complete Mini]. After electrophoresis (SDS/PAGE gel), the proteins were transferred to nitrocellulose membrane, and the membrane was incubated with the appropriate primary antibody including the following: p21 (Santa Cruz; F-5; sc-6246), $p16^{INK4a}$ (Santa Cruz; M-156; sc-1207), $p19^{ARF}$ (Abcam; s-C3; 26696), p53 (Santa Cruz; DOI; sc-126), p53 (Novocastra; CM-5; NCL-p53-CM5p), γH2Ax-(ser139) (Upstate/Millipore; 07-164), anti-TK2 (Primm), OXPHOS complexes (Mitosciences; MS-604), Porin (Mitosciences; MS-A03), C-I NDUFB8 (Mitosciences; MS-105), C-IV Sub1 (Mitosciences; MS404), C-II Sub.30kDa (Mitosciences; MS-203), C-II Sub.70kDa (Mitosciences; MS-204), ATP synthase (C-V) (Mitosciences; MS-502), C-IV Sub2 (Mitosciences; MS405), C-IV Sub4 (Santa Cruz; 20E8; sc-58348), NDUFA9 (Santa Cruz; 20C11; sc-58392), anti-Porin (Calbiochem; Ab-5; PC548), and β-actin (Sigma; AC-15; A5441). Protein–antibody interactions were detected with a peroxidase-conjugated secondary antibody, subjected to Pierce ECL Chemiluminescent reagent, and when indicated using the Odyssey imaging system (LI-COR). Secondary antibodies were from Amersham (ECL) or Pierce (Odyssey).

Immunocytochemistry. For immunocytochemistry experiments, cells were fixed with 4% (vol/vol) paraformaldehyde in PBS, pH 7.4, for 10 min at room temperature. Excess buffer was drained, and the cells were washed three times in PBS. Cells were then permeabilized using 0.1% Triton X-100 in PBS with 3% (vol/vol) BSA. Fixed cells were incubated with the appropriate primary antibody in PBS with 10% (vol/vol) goat serum and 0.1% Triton X-100 overnight at 4 °C. Antibodies against the following antigens were used: γH2Ax-(ser139) (Upstate/Millipore; JBW301; 05-636), GFAP (DAKO; Z0334), Nestin (Abcam; ab11306), and Olig-2 (Millipore; 9610). Cells were washed and incubated with anti-mouse or anti-rabbit Alexa-conjugated antibodies (Alexa Fluor; Invitrogen) for 1 h at room temperature. Coverslips were washed and mounted. All imaging was performed on a Zeiss Axiovert 200M (Carl Zeiss) microscope using a 20×, 40×, or a 63× objective.

RNA Extraction and Quantitative Real-Time PCR. Total RNA was derived from cells using the Qiagen RNAeasy kit (Qiagen) and tested for purity (A260/280 ratios) and integrity (denaturing gel electrophoresis). Quantitative real-time PCR (qPCR) amplification was performed using specific primers for mouse or human (SYBR Green; Applied Biosystems). Thermal cycling was performed using the ABI PRISM 7000 Sequence Detector System (AB).

Cell Cycle and Reactive Oxygen Species Expression Analysis. Samples for cells cycle analysis were collected over the indicated time points and fixed in 70% (vol/vol) ethanol overnight. Fixed cells were treated with RNase for 20 min before addition of 5 μg/mL propidium iodide (Sigma; P4864) and analyzed by FACS (CyAn ADP; DAKO). For reactive oxygen species (ROS) intracellular quantification and mitochondrial mass analysis, NPCs were recollected using accutase and washed two times in PBS before incubating with 5 μM hydrogen peroxide-sensitive dye dichlorofluorescein (DCFDA) (Invitrogen; C369) or nonyl acridine orange (NAO) (Invitrogen; A1372) for 15 min at 37 °C. The samples were then washed two times in PBS before performing flow-cytometric analysis.

Derivation of Cultured Human Cells GNS from Surgical Biopsies. All patients have given informed consent before the surgical intervention. The storage of human tissue is governed by the Human Tissue Act (United Kingdom; HTA License 12054). The use of tissue and cells has been approved by the National Hospital Ethics Committee (LREC 08/0077). Neurosurgical biopsies were obtained at the operating theater and immediately transferred into the Department of Neuropathology, where they were dissected for tissue processing into paraffin blocks and subsequent histopathological examination and a further portion was snap frozen. To prepare cells, a third portion was minced as finely as possible and suspended in cold PBS. Erythrocytes were lysed in ACK buffer (Invitrogen) when necessary. Tissue fragments were trypsinized, triturated, and transferred into six-well plates with medium containing Brain Tumor Initiating Cell (BTIC) permissive medium (DMEM/Ham F12; 15 mM Hepes; L-glutamine; pen/strep, 10 kU/10 mg/mL), B27 Supplement (Invitrogen; 17504-044), EGF (recombinant mouse; PeproTech; 315-09; 20 ng/mL), bFGF (recombinant human; PeproTech; 100-18B; 20 ng/mL). For the first week, cells were cultured free floating to form spheres and subsequently transferred into laminin-coated dishes (Sigma; L2020; 0.01 mg/mL), in which they grow adherently. G1 (69-y-old male), G2 65-y-old male), G3 (60-y-old female), G4 (76-y-old female), G144 (51-y-old male), and G166 (74-y-old female) were diagnosed as classic glioblastoma (GBM). G144 and G166 were derived by Steve Pollard and colleagues in Peter Dirks's Laboratory (University of Toronto, Toronto, ON, Canada) (1). Cell were grown at 37° C, 95% (vol/vol) rH, 20% (vol/vol) O_2, and 5% (vol/vol) CO_2. GNS cells were routinely grown to confluence, dissociated using accutase (Sigma; A6964), and then split 1:3–1:5. Medium was replaced every 3–5 d.

Human Fetal Neural Stem Cell Culture. Human fetal brain Cb660 were derived by Yirui Sun, Steve Pollard, and colleagues (2) in Austin Smith's Laboratory (University of Cambridge, Cambridge, UK) under ethical approval from the Lothian Healthcare Trust using tissue donated with informed consent after elective termination of pregnancy. Human NS cell lines were maintained onto laminin (10 mg/mL; Sigma)-coated dishes in expansion media (RHA-B media from Stem Cell Sciences supplemented with 10 ng/mL of both bFGF and EGF). Medium was changed every 2 d, and cells were split 1:2–1:3 once the culture became confluent.

Measurement of 8-Hydroxy-2′-deoxyguanosine. After protein fractionation, nuclear DNA was extracted using a QIAamp DNA Mini Kit (Qiagen) and digested with nuclease P1. A commercially available ELISA kit from StressMarq Bioscience was used to determine levels of 8-hydroxy-2′-deoxyguanosine (8-OHdG) in isolated DNA. The assays were performed according to the manufacturer's instructions. The 8-OHdG standard (0.0103–30 ng/mL) or 0.5-μg DNA from cells was incubated with an anti-mouse IgG-coated plate with a tracer consisting of an 8-OHdG–enzyme conjugate. The assay was normalized by an equal amount of DNA used for each sample. Addition of a substrate to replicate samples was followed by measurement of absorbance at 415 nm. Standard curves were calculated for all reactions with serial dilutions of 8-OHdG standard to calculate reaction efficiency. Samples were assayed in triplicate.

Animal Studies. Animals were kept according to institutional and United Kingdom Home Office guidelines (Project License 70/6603). NOD/SCID mice (Harlan) and C57BL/6×FVB mice were kept in groups of four mice per cage and were bred in-house. Cell transplantations were done by injecting ∼5 μL of the tumor sphere suspension (containing ∼1,000 neurospheres or 1×10^6 cells) into the left striatum of 6-wk-old recipient mice (bregma, 1.5 mm lateral, 2 mm deep), using a 22-gauge needle attached to a 25-μL Hamilton syringe (RN1702).

Histological Examination. Brains were fixed in 10% (vol/vol) formalin, embedded in paraffin, cut into 3-μm sections, and processed for H&E staining. On representative tumors, antibodies or antisera against the following antigens were used: GFAP (DAKO; Z0334), Nestin (Abcam; ab11306), Sox2 (Chemicon/Millipore; ab5603), and Olig-2 (Millipore; 9610). All immunostaining was carried out using the automated Ventana Discovery (Ventana Medical Systems) apparatus following the manufacturer's guidelines, using biotinylated secondary antibodies and a horseradish peroxidase-conjugated streptavidin complex and diaminobenzidine as chromogen.

shRNA Mouse Lentivectors. To knockdown TK2 and NDUFA10 expression in NPCs, we used the commercially available pGIPZ-lentiviral shRNAmir vectors containing a hairpin sequence targeting *TK2* or *NDUFA10* (Open Biosystems). The *TK2* hairpin sequence was as follows, with underlined sequencing corresponding to region of the mouse TK2 gene targeted: TGCTGTTGACAGTGAGCGCGCTGCTCTTGACATTCTAGAATAGTGAAGCCACAGATGTATTCTAGAATGTCAAGAGCAGCATGCCTACTGCCTCGGA. The *NDUFA10* hairpin sequence was as follows, with underlined sequencing corresponding to region of the mouse NDUFA10 gene targeted: TGCTGTTGACAGTGAGCGCAGGTGGTAGAGGACATTGAATAGTGAAGCCACAGATGTATTCAATGTCCTCTACCACCTATGCCTACTGCCTCGGA. The shRNA-containing lentiviral vector was cotransfected with lentiviral packaging into HEK-293T cells (Open Biosystems) to produce shRNA-carrying lentivirus particles. Culture supernatants were collected at 48 h after transfection, and lentivirus particles were concentrated using PEG (System Biosciences). NPCs were transduced by the resulting concentrated viral particles (multiplicity of infection of 10) for 1 h and after that immediately supplemented with fresh media.

Retroviral Expression of Tp53 and Ires-GFP. Mouse Tp53 variant 1 was initially cloned in a pCRII-Topo vector (Invitrogen) and subsequently transferred into the BamHI/EcoRI sites of pBabe GFP (Addgene plasmid 10668). A PCR-amplified fragment containing Tp53 variant1-HA-specific C terminus was cloned into the SacII/EcoRI sites of the p53-pBabe GFP to obtain the pBabe WTp53-HA GFP vector. Retroviral plasmid, pBabe WTp53-HA GFP, pBabe GFP, MSCV IRES-GFP, and MSCV hRASv12 IRES-GFP (Addgene plasmids 20672 and 18780, respectively) were used for the production of high-titer retroviral supernatants. Culture supernatants were collected at 36 h after transfection, and retroviral particles were concentrated using a PEG-it technology [System Biosciences (SBI)]. NPCs were transduced by the resulting concentrated viral particles for 1 h. Infected cells were selected after 4 d using an air-in-jet high-speed cell sorter (MoFlo).

Statistical Analysis. All experiments were performed in triplicate for each condition and from at least three different cell culture preparations. Results are expressed as mean ± SD or SEM where indicated. Statistical analysis was performed by one-way ANOVA with Bonferroni posttest to compare all conditions or by paired or unpaired Student's *t* test using Prism 5.0 software (Graph Pad Software). Values of $P < 0.05$ were regarded as significant.

1. Wallace DC (2005) A mitochondrial paradigm of metabolic and degenerative diseases, aging, and cancer: A dawn for evolutionary medicine. *Annu Rev Genet* 39:359–407.

2. Viros A, et al. (2014) Ultraviolet radiation accelerates BRAF-driven melanomagenesis by targeting TP53. *Nature* 511(7510):478–482.

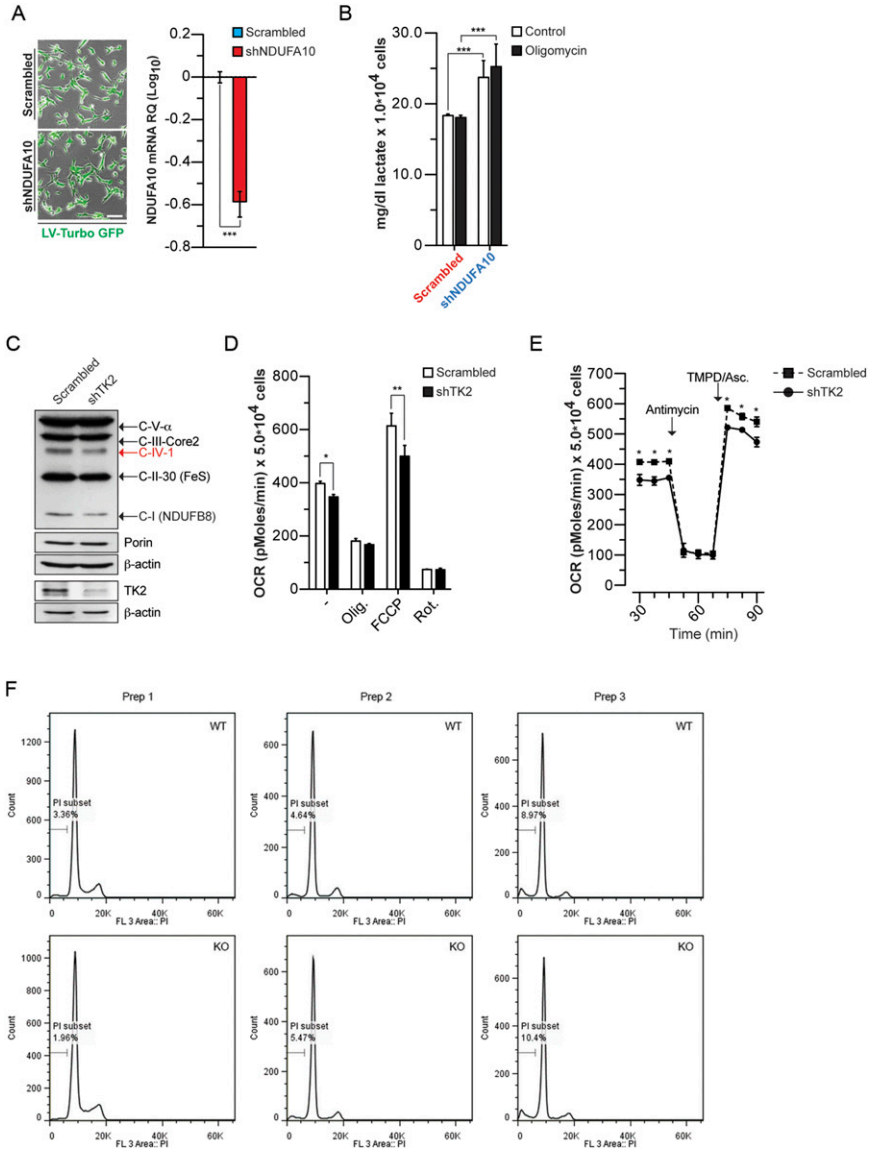

Fig. S1. (*A*) Representative images of WT NPCs infected with Lentiviral Turbo-GFP shRNA vectors expressing a shRNA sequence targeting the complex I subunit NDUFA10 [nuclear-DNA encoded proteins; NADH dehydrogenase (ubiquinone) 1α subcomplex, 10 of complex I] or a scrambled sequence. [Scale bar: 20 μm (*Left*).] QPCR expression analysis of NDUFA10 (*Right*). Approximately 75% reduction of NDUFA10 mRNA is observed in shNDUFA10-transduced NPCs ($n = 3$; $^{***}P < 0.0001$, Student's *t* test; data are represented as mean ± SEM). (*B*) Lactate production in Scramble and shNDUFA10-transfected NPCs. Lactate production was measured under basal conditions or after oligomycin treatment. (*C*) Levels of ETC proteins (in red mtDNA-encoded proteins) at steady state using an antibody mix against OXPHOS complexes in NPCs transduced with shRNA vector expressing a shRNA sequence targeting TK2 or a scrambled sequence. Porin and β-actin are shown as loading controls for mitochondria and total protein extracts, respectively. (*D*) Oxygen consumption rate (OCR) in NPCs transduced with shRNA for TK2 under basal conditions, following the addition of the mitochondrial inhibitor oligomycin (0.1 $\mu g \cdot mL^{-1}$), in the presence of the uncoupler FCCP (0.4 μM), in the presence of complex I inhibitor rotenone (0.2 μM) or the complex IV substrates TMPD/ascorbate (0.5 mM/2 mM). OCR was measured using the XF24 SeaHorse Analyzer (Seahorse Bioscience). (*E*) Complex IV respiratory capacity using antimycin and TMPD/ascorbate. Data are average of three independent experiments as mean ± SEM. $^{*}P < 0.05$, $^{**}P < 0.01$. (*F*) Subdiploid peak analysis of WT and KO cells fixed and stained with propidium iodide. Three independent preparations are shown. Percentages of apoptotic cells displaying subdiploid DNA content are indicated in the figure panels.

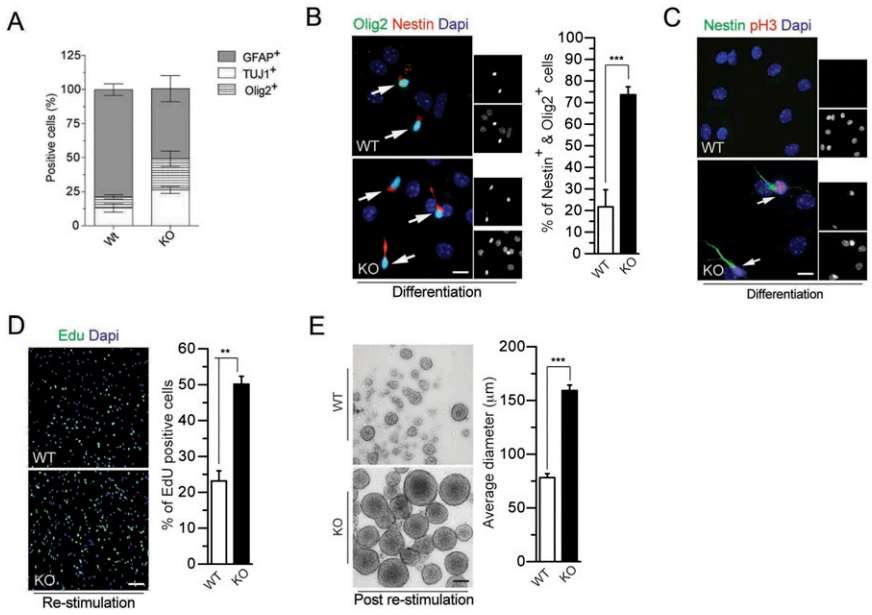

Fig. S2. Altered differentiation properties of KO NPCs. NPCs were differentiated by sequential removal of growth factors in defined differentiation medium (3 d without EGF, followed by 5 d without any growth factors). KO NPCs are able to generate the three main neural lineages ($GFAP^+$ astrocytes, $Tuj1^+$ neurons, and $RIP^+/Olig2^+$ oligodendrocytes). (*A* and *B*) KO cultures display increase number of differentiation-resistant NPCs, which are positive for the NPC markers Olig2 ($n = 3$; $^{***}P < 0.001$, Student's *t* test). (*C*) A subset of $Nestin^+$ cells are also positive for the mitotic marker phospho-histone 3 (pH3). (*D*) EdU incorporation assays show that a larger number of KO NPCs evade differentiation and can reenter cell cycle if restimulated with full proliferation medium ($n = 3$; $^{**}P < 0.01$, Student's *t* test). (*E*) Proliferation of NPCs after restimulation was measured using the neurosphere assay. Neurosphere diameter is increased in restimulated KO NPCs ($n = 3$; $^{***}P < 0.0001$, Student's *t* test). (Scale bar: 10 and 100 μm.)

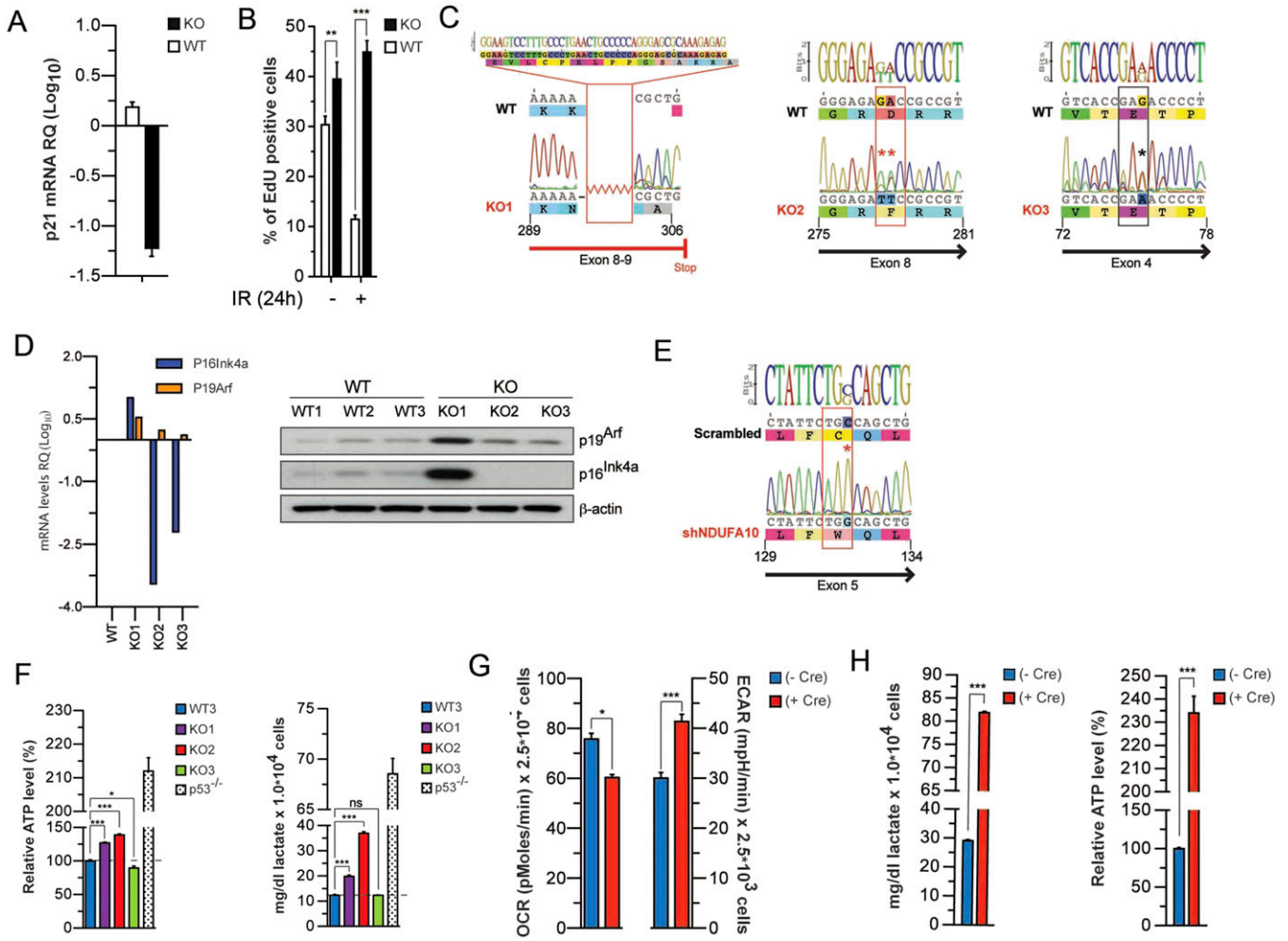

Fig. S3. (*A*) QPCR analysis of the cyclin-dependent kinase inhibitor (CKi) p21^{WAF1} (p21) in WT (WT1) and KO (KO1) NPCs. β-Actin was used as a loading control. (*B*) Ionizing irradiation (gamma-IR)-induced Unscheduled DNA Synthesis (UDS) in WT and KO NPCs. WT and KO NPCs were cultured on laminin-coated coverslips and treated with gamma IR (2 Gy·min^{-1}). Cells were treated with EdU (5 mM) for 2 h before paraformaldehyde (PFA) fixation. For each data point, at least 250 nuclei were analyzed (data represent mean and SD; $n = 3$; $^{**}P < 0.01$, $^{***}P < 0.001$). (*C*) DNA sequence analysis and chromatogram of the p53 gene in metabolically adapted KO cells. The figures show the region containing the p53 mutations identified in in KO2, KO3 cells, and a 44-bp nucleotide deletion in KO1 cells. WT sequence is provided as reference. (*D*) QPCR (*Left*) and Western blot (*Right*) analyses showing expression of p19^{arf} and p16^{Ink4a} protein and mRNA levels in WT and TK2 KO (KO) different NPCs preparations. β-Actin was used as a loading control. (*E*) DNA sequence analysis and chromatogram of the p53 gene in metabolically adapted shNDUFA10 cells compared with scramble sequence transduced NPCs. (*F*) ATP levels (*Left*) and lactate production (*Right*) in WT, TK2 KO, and p53 KO NPC preparations ($n = 3$; data are represented as mean ± SEM; $^{*}P < 0.05$, $^{**}P < 0.01$, $^{***}P < 0.001$). (*G*) Basal oxygen consumption rate (OCR) (*Left*) and extracellular acidification rate (ECAR) (*Right*; data represent mean and SD; $n = 3$; $^{*}P < 0.05$, $^{***}P < 0.001$). Lactate production (*H*) and relative ATP levels (*H*) in p53$^{flox/flox}$ NPCs recombined (+Cre) or not (Cre−) (data represent mean and SD; $n = 3$; $^{***}P < 0.001$).

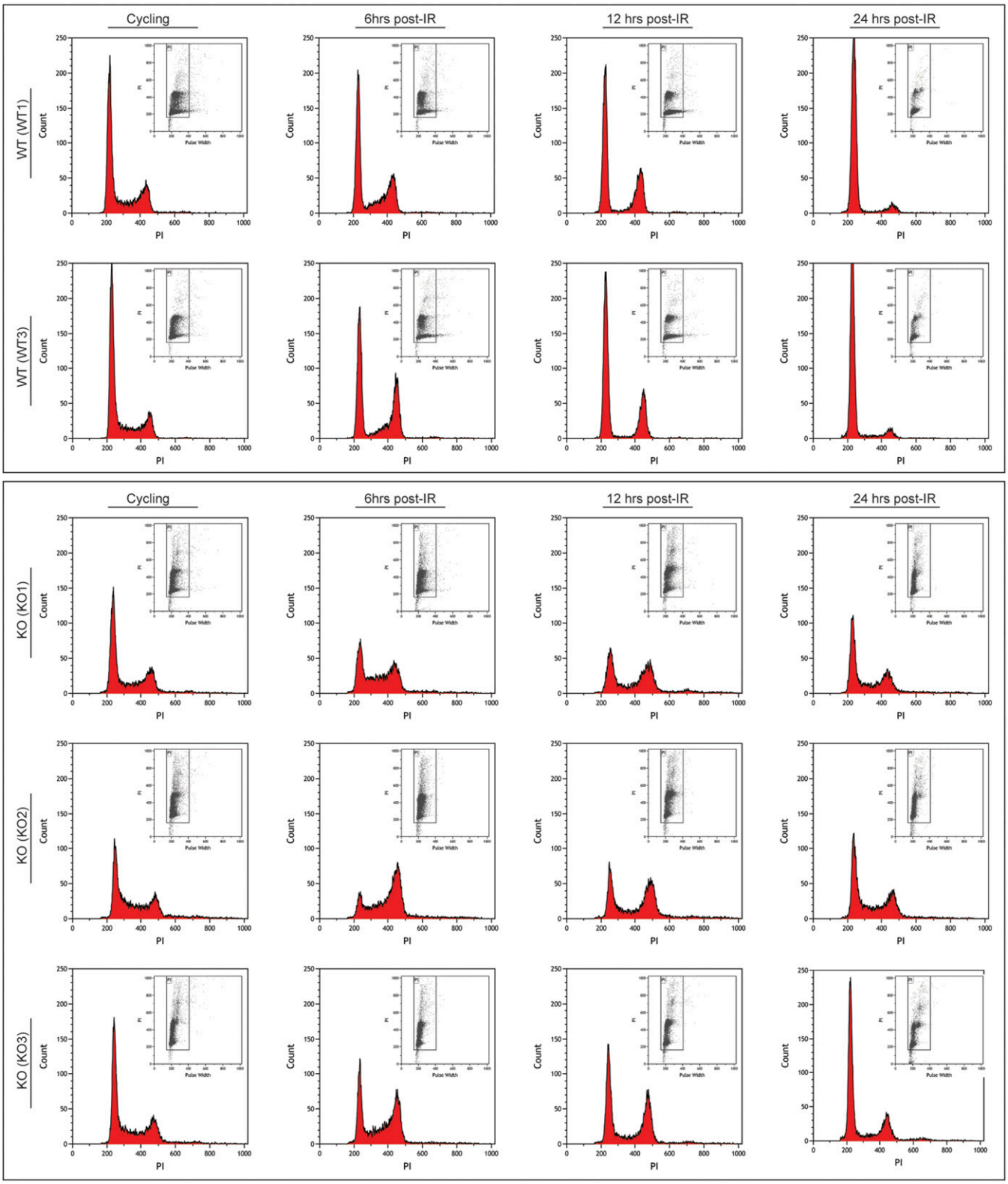

Fig. S4. Analysis of WT (two preparations) and TK2 KO cells (three different preparations) basal cell cycle using propidium iodide incorporation (Fig. S2) at different time points (6, 12, and 24 h) after gamma irradiation (2 Gy·min^{-1}).

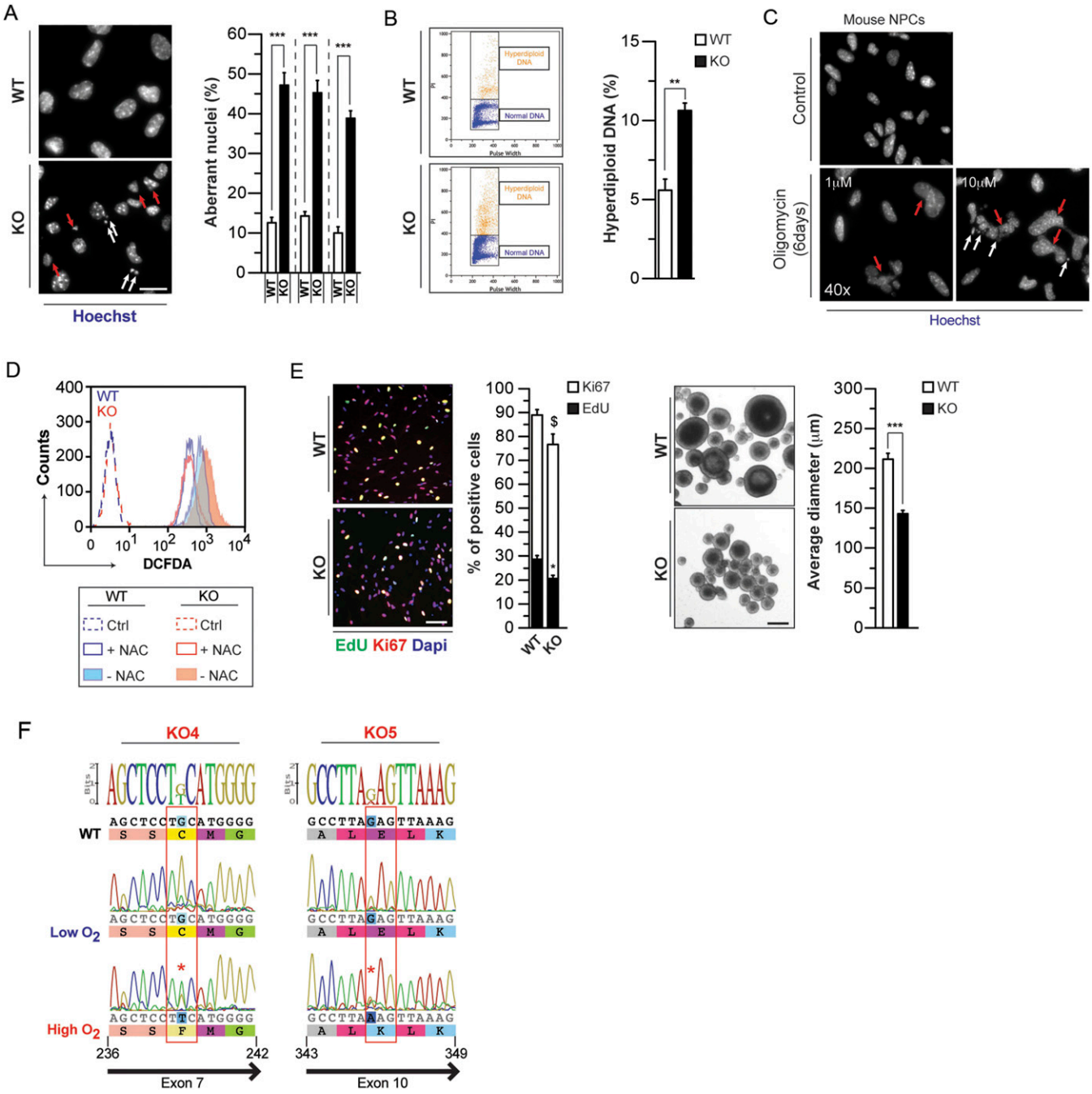

Fig. S5. (*A*) Analysis and quantification of nuclear morphology in wild-type (WT) and TK2 KO (KO) NPCs. TK2 KO NPCs display aberrant nuclear morphology (red arrows) and micronuclei (white arrows; $n = 3$ independent preparation; Table S1). (*B*) Analysis of hyperploid DNA content in early passages of WT and Tk2 KO cells. Representative plots of FACS analysis for hyperploid DNA content are shown (*Left*) as well as bar graph showing the percentage of cells with hyperdiploid DNA content (*Right*) (data are represented as mean ± SEM; $^{**}P < 0.01$, $^{**}P < 0.01$). (*C*) Analysis of nuclear morphology in WT NPCs treated for 6 d with oligomycin or vehicle. Oligomycin-treated NPCs display aberrant nuclear morphology (red arrows) and micronuclei (white arrows; $n = 3$ independent experiments). (*D*) ROS levels quantification in WT and TK2 KO NPCs with or without the antioxidant NAC (0.1 mM). (*E*) Proliferation of NPCs was studied using EdU labeling (2-h incubation) and immunodetection of Ki67. Graph shows quantification of EdU and Ki67. (Scale bar: 40 μm.) (Data are represented as mean ± SEM; $n = 3$; $^{***}P < 0.001$, $^{**}P < 0.01$, and * or $^{\$}P < 0.05$.) For the neurosphere assay (*Right*), at least 200 spheres for each genotype were counted. (Scale bar corresponds to 100 μm.) (*F*) DNA sequence and chromatogram of p53 gene in KO cells grown in high- (normoxia, 21% O_2) or low-oxygen (moderate hypoxia, 2.5% O_2) conditions. Mutations identified in two of the preparations grown in high oxygen are shown. No mutation was detected in cells grown in low oxygen.

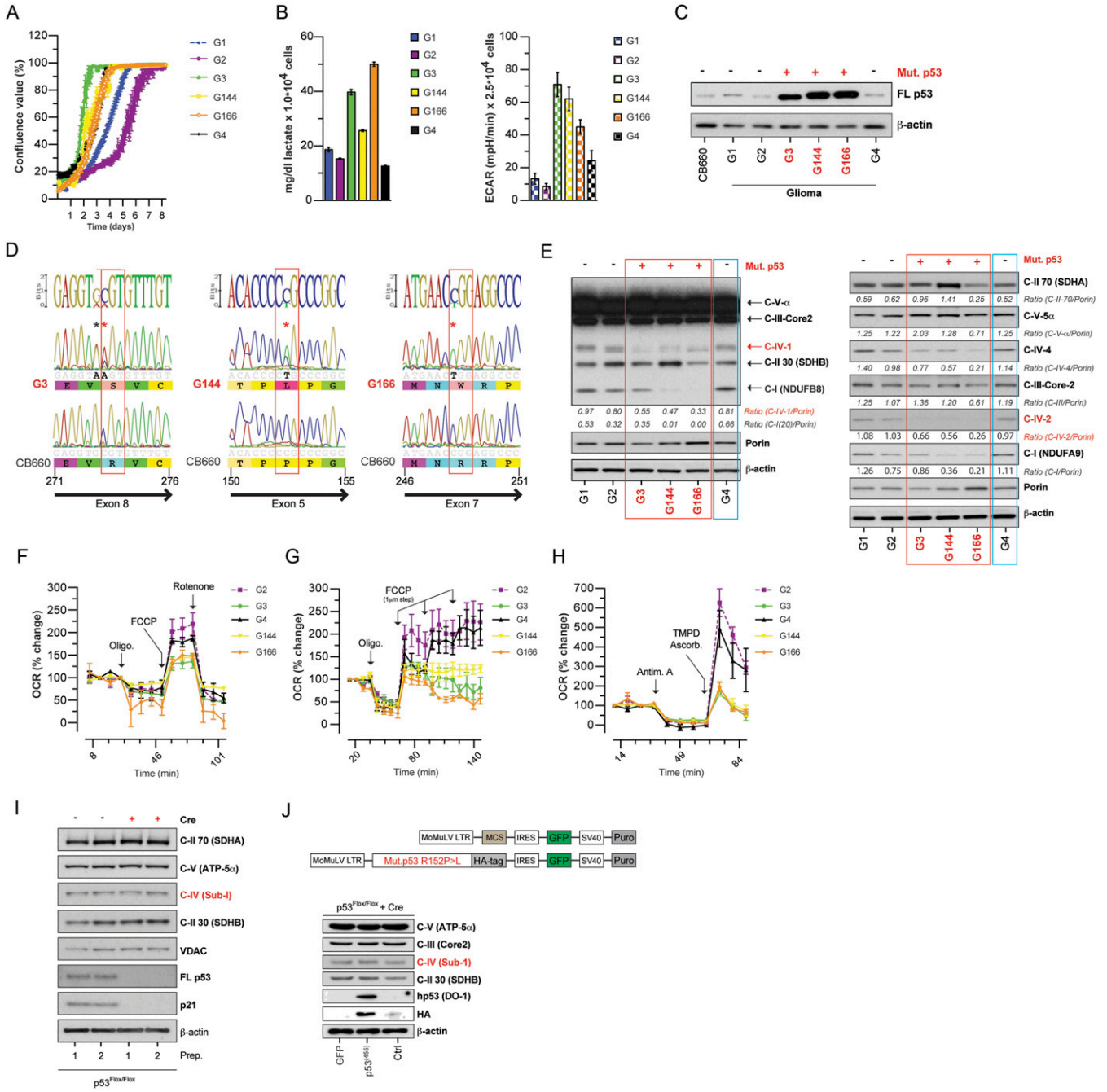

Fig. S6. (*A*) Proliferative capacity of human glioma neural stem cells (GNSs) derived from primary human glioblastoma multiforme (G1, G2, G3, G4, G144, G166) measured using High Definition (HD) imaging system (INCUCYTE Live-Cell Imaging System). (*B*) Lactate production (*Left*) and extracellular acidification rate (ECAR) (*Right*) of GNSs under basal conditions. (*C*) Representative immunoblot analysis of p53 in GSC; β-actin was used as a loading control. (*D*) Representative DNA sequence and chromatogram analysis of the human p53 gene. Mutations of p53 gene in G3, G144, and G166 cells are highlighted in red. p53 sequence in CB660 cells (control human fetal NS) is provided as reference. (*E*) Levels of ETC proteins (in red, mtDNA-encoded proteins; in black, nuclear-encoded proteins) and relative quantification. Porin and β-actin are shown as loading controls for mitochondria and total protein extracts, respectively. (*F–H*) Oxygen consumption rate (OCR) of GNSs following the addition of the mitochondrial inhibitor oligomycin (0.1 $\mu g \cdot mL^{-1}$), the uncoupler FCCP (0.4 mM), and complex I inhibitor rotenone (0.2 mM) (*F* and *G*) or the complex IV substrates TMPD/ascorbate (0.5 mM/2 mM; see *H*). OCR was measured using the XF24 SeaHorse Analyzer (Seahorse Bioscience). Data are average of three independent experiments as mean ± SEM. (*I*) Representative Western blot of respiratory chain complexes in $p53^{flox/flox}$ NPCs recombined (+Cre) or not (Cre−). β-Actin and Porin have been used as a loading controls. (*J*) Representative Western blot of respiratory chain complexes in $p53^{flox/flox}$ NPCs recombined (+Cre) transduced with a plasmid containing a mutated isoform of p53 (p53 R152P > L) or GFP empty vector. Untransduced recombined (+Cre) $p53^{flox/flox}$ NPCs have been used as control. β-Actin has been used as a loading control.

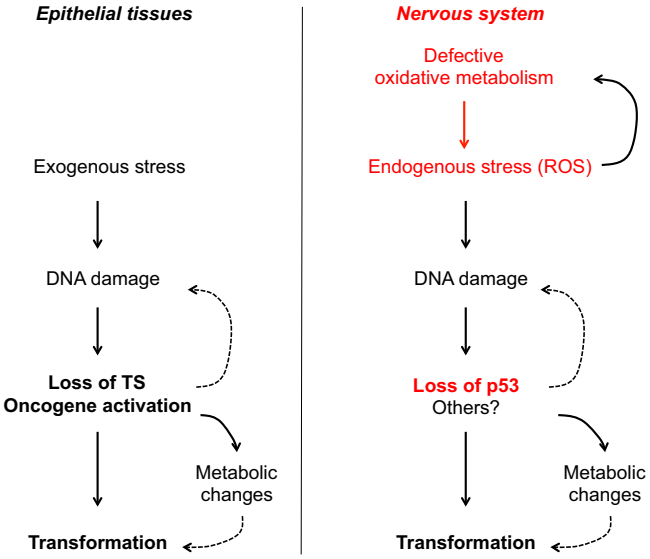

Fig. S7. In epithelial tissues exogenous stress can lead to transformation via genetic loss of tumor suppressors or oncogenic activation. In contrast, in the nervous system endogenous stress caused by mitochondrial dysfunction can fuel transformation via loss of the p53 tumor suppressor, which in turn can promote additional metabolic changes with potential transforming function. In both scenarios, loss of tumor suppressive control or oncogenic activation can increase genome instability while at the same time promoting further metabolic changes that can contribute to transformation. Finally, ROS can promote a vicious circle leading to more mitochondrial damage. Loss of p53-mediated DNA damage checkpoints may also increase DNA damage.

Table S1. List of WT and KO NPC preparations with indicated time of switch to glycolysis and increased growth

Prep ID used in this study	Genotype	Passage	Glycolytic switch	Growth	p53 mutation	Comments	Internal prep ID code
WT1	WT	Up to P14	No	No	No	Genomically stable	W1
WT2	WT	Up to P12	No	No	No	Genomically stable	W2
WT3	WT	Up to P12	No	No	No	Genomically stable	W3
	WT	Up to P7	No	No	No	Genomically stable	W4
WT5	WT	Up to P6	No	No	No	Genomically stable	W5
WT4	WT	Up to P8	No	No	No	Genomically stable	WT_HO
KO1	KO	P7	Yes	+++	Yes	Deletion	D1
KO2	KO	P5	Yes	+++	Yes	R.278F	C1
KO3	KO	P6	No	—	Yes	R.73E (conservative)	G1
	KO	P12	ND	+++	Yes		F1
	KO	Up to P5	ND	+	ND	ND	H1
KO4	KO	P6	ND	+++	Yes	R.239F	XK1
KO5	KO	P5	Yes	++	Yes	R.346K	KO_HO
Scrambled	WT	Up to P8	No	No	No	Genomically stable	SW3
shNDUFA10	WT (siRNA)	P5	Yes	+	Yes	R.132W	shNDUFA10
	WT	Up to P4	No	No	No	Genomically stable	WT1_HO
	WT	Up to P4	No	No	No	Genomically stable	WT3_HO
	WT	Up to P4	No	No	No	Genomically stable	WT2_HO
WT4	WT	P0	ND	ND	ND	Genomically stable	WT4
WT5	WT	P0	ND	ND	ND	Genomically stable	WT5
WT6	WT	P0	ND	ND	ND	Genomically stable	WT6
WT8	WT	P0	ND	ND	ND	ND	WT8
WT9	WT	P0	ND	ND	ND	ND	WT9
WT10	WT	P0	ND	ND	ND	ND	WT10
	KO	Up to P4	ND	++	ND	Aberrant nuclei	A2
	KO	P0	ND	ND	No	Aberrant nuclei	A4
	KO	Up to P4	No	No	No	Aberrant nuclei	KO1_HO
	KO	Up to P4	No	No	No	Aberrant nuclei	KO3_HO
	KO	Up to P4	No	No	No	Aberrant nuclei	KO2_HO
KO5	KO	P0	ND	ND	ND	Aberrant nuclei	KO5
KO6	KO	P0	ND	ND	ND	Aberrant nuclei	KO6
KO7	KO	P0	ND	ND	ND	Aberrant nuclei	KO7
KO8	KO	P0	ND	ND	ND	ND	KO8
KO9	KO	P0	ND	ND	ND	ND	KO9
KO10	KO	P0	ND	ND	ND	ND	KO10

Table S2. Information related to the tumor study

Animal ID	Genotype	Sex	Exp. start	Incubation, d	Incubation, d	CoD	Tumor, Y/N	Tumor size	Necrosis	Comments
402367	C57/B6	F	4/14/11	75	KO/IRES	Timed cull	Y	T1	N	Scar
395747	C57/B6	F	4/14/11	150	KO/IRES	Culled end of exp.	N	0		Scar
395748	C57/B6	F	4/14/11	150	KO/IRES	Culled end of exp.	N	0		Scar
395754	C57/B6	M	4/14/11	150	KO/IRES	Culled end of exp.	N	0		No lesion
395755	C57/B6	M	4/14/11	150	KO/IRES	Culled end of exp.	N	0		Scar
395750	C57/B6	M	4/14/11	75	WT/IRES	Timed cull	N	0		Scar
395749	C57/B6	F	4/14/11	150	WT/IRES	Culled end of exp.	N	0		Scar
395751	C57/B6	M	4/14/11	150	WT/IRES	Culled end of exp.	N	0		Scar
395752	C57/B6	M	4/14/11	150	WT/IRES	Culled end of exp.	N	0		Scar
395753	C57/B6	M	4/14/11	150	WT/IRES	Culled end of exp.	N	0		Scar
426726	C57/B6	F		117	KO	Timed cull	Y			
426716	C57/B6	M		173	KO	Culled end of exp.	N			
426717	C57/B6	M		173	KO	Culled end of exp.	N			
426718	C57/B6	M		173	KO	Culled end of exp.	N			
426719	C57/B6	M		173	KO	Culled end of exp.	N			
426723	C57/B6	M		98	WT	Timed cull	N			
426721	C57/B6	M		164	WT	Culled end of exp.	N			
426722	C57/B6	M		173	WT	Culled end of exp.	N			
426724	C57/B6	M		173	WT	Culled end of exp.	N			
426725	C57/B6	M		146	WT	Timed cull	N			
402513	NOD_SCID	F	4/14/11	0	KO/IRES	Woke up ataxic, culled sample taken	N	0		—
402515	NOD_SCID	M	4/14/11	42	KO/IRES	Culled sick	Y	T3	N	
402514	NOD_SCID	M	4/14/11	150	KO/IRES	Culled end of exp.	N	0		Scar
402516	NOD_SCID	M	4/14/11	150	KO/IRES	Culled end of exp.	N	0		Scar
401451	NOD_SCID	F	4/14/11	75	WT/IRES	Timed cull	N	0		Scar
401452	NOD_SCID	F	4/14/11	150	WT/IRES	Culled end of exp.	N	0		No lesion
401453	NOD_SCID	F	4/14/11	150	WT/IRES	Culled end of exp.	N	0		Scar

Dataset S1. Heat map of statistically significant biochemical products profiled in this research

Dataset S1